JOURNAL OF MATERIALS SCIENCE 16 (1981) 1748–1756

The effect of dissolution on the growth of the Fe_2Al_5 interlayer in the solid iron - liquid aluminium system

V. N. YEREMENKO, Ya. V. NATANZON, V. I. DYBKOV
Institut Problem Materialoznavstva, Kiev 252142, USSR

Using both a parabolic law for crystal growth and an exponential law for dissolution of solids in liquids, an equation describing the diffusion-controlled growth of a single-phase intermetallic layer has been derived. This equation enables calculation of the interlayer thickness as a function of time under given conditions of interaction of a solid metal with a liquid one. The growth rate of the Fe_2Al_5 interlayer follows the predicted time dependence.

1. Introduction

The formation of a brittle-layered intermetallic phase during the interaction of a solid metal with a liquid one (examples include hot-dip coating, soldering, built-up welding, etc.) results in a sharp deterioration of the joints mechanical properties and hence it is necessary to use interaction conditions which prevent the formation of thick intermetallic layers. Obviously, the interlayer thickness can be reduced by increasing the solid metal dissolution rate. It seems at first sight that at a certain dissolution rate, the interlayer would disappear completely; more thorough analysis shows that this initial conclusion is not the case, at least in the case where atomic diffusion is the rate-controlling step during growth of the interlayer.

In most cases of practical interest it is necessary to know the maximum possible vlaue of the interlayer thickness under given conditions of the solid metal–liquid interaction. The purpose of the present work is to answer this and related questions.

The Fe–Al system was selected for study because of its practical applications and because of the convenient experimental conditions which can be used to check the theoretical predictions.

2. Theory

2.1. Dissolution of a solid metal in a liquid metal

The dissolution of a solid metal in a liquid metal is described either by the equation

$$\frac{dc}{dt} = k\frac{s}{v}(c_s - c) \tag{1}$$

or by the integrated form (initial condition: $c = 0$ at $t = 0$)

$$c = c_s\left[1 - \exp\left(-\frac{kst}{v}\right)\right], \tag{2}$$

where c is the concentration of the dissolved metal in the bulk of the melt measured at time, t, c_s is the saturation concentration, k is the dissolution rate constant, s is the specimen surface area and v is the melt volume.

Equation 1 was proposed to describe the dissolution of solids in liquids by Shchukarev in 1896, Noyes and Witney in 1897, Brunner in 1904 and Nernst in 1904, but it was Nernst who laid the principles of the dissolution theory [1]. According to the Nernst theory, the dissolution rate constant can be written as follows

$$k = \frac{D}{\delta}, \tag{3}$$

where D is the diffusion coefficient of the dissolved metal and δ is the thickness of the diffusion boundary layer. Naturally, in this case the dissolution process is regarded to be diffusion controlled, i.e. the diffusion of the solute atoms through the diffusion boundary layer is the rate-determining step during dissolution.

Note that, for well-stirred systems, Equation

0022–2461/81/071748–09$02.90/0

1 follows immmediately from Fick's first law [1]. Indeed, in this case the concentration of the dissolved metal may be considered to be uniform everywhere in the bulk of the melt at any time, except for the region of the diffusion boundary layer, in which the concentration increases almost linearly with distance in the direction normal to the solid–liquid interface from the bulk value up to the saturation concentration, so that

$$\frac{\partial c}{\partial x} = \frac{c - c_s}{\delta}. \quad (4)$$

Inserting this expression into Fick's first law gives the flow j as

$$j = \frac{D}{\delta}(c_s - c). \quad (5)$$

Taking into account that the flow, j, can be written as

$$j = \frac{v}{s}\frac{dc}{dt} \quad (6)$$

then Equation 1 is obtained.

Further refinement of the dissolution theory enables the thickness of the diffusion boundary layer to be calculated. For a rotating disc, the surface of which is equally accessible from the view-point of diffusion

$$\delta = 1.61 D^{1/3} \nu^{1/6} \omega^{-1/2}, \quad (7)$$

where ν is the kinematic viscosity of the melt and ω is the angular speed of disc rotation [2].

Hence, from Equation 3

$$k = 0.62 D^{2/3} \nu^{-1/6} \omega^{1/2}. \quad (8)$$

This equation is valid if the Schmidt number, Sc, ($Sc = \nu/D$) exceeds 1000, but in the liquid–metal systems $Sc < 1000$. This is why the following expression appears to be preferable:

$$k = 0.554 I^{-1} D^{2/3} \nu^{-1/6} \omega^{1/2}, \quad (9)$$

where $I = f(Sc)$ [3]. Equation 9 is applicable for $Sc > 4$.

2.2. Growth of the interlayer

The process being analysed is the formation of an intermetallic compound, AB, at the interface between a higher melting-point solid, A, and a liquid, B, see Fig. 1.

There are two simultaneous processes taking place. Firstly, the interlayer growth as the A and B atoms diffuse across the AB layer in the opposite

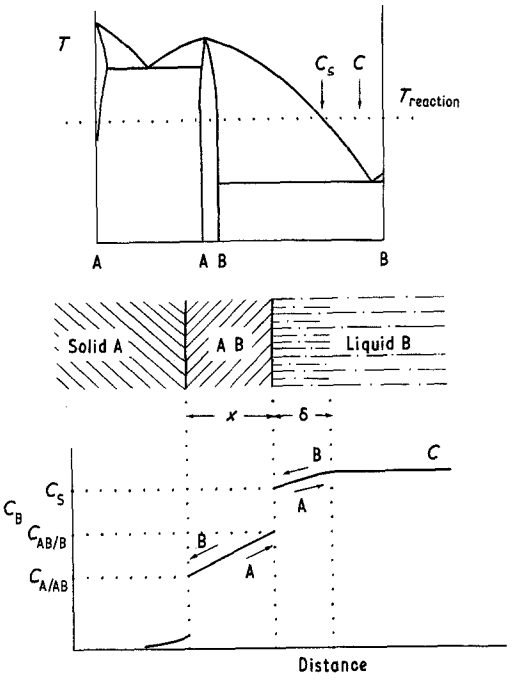

Figure 1 Schematic diagram to illustrate the growth and dissolution of an intermetallic compound AB at the solid–liquid interface.

directions and react at the AB–B and A–AB interfaces to form more intermetallic, AB. Secondly, the dissolution of AB into the liquid to feed the refractory metal A into the liquid which is undersaturated with A.

There are therefore three interfaced velocities:

(a) The movement of the AB–B interface, say, to the right as A atoms diffuse across AB towards the AB–B interface and react with B atoms.

(b) The movement of the A–AB interface to the left as B diffuses towards this interface and reacts with A. Here we shall consider the total growth of the interlayer, but not the partial one to the right and to the left separately. It should also be noted that the interlayer is assumed to be present at the A–B interface from the very beginning of the solid–liquid interaction and hence the early (kinetic) stage of its growth is outside the scope of our consideration.

(c) The movement of the AB–B interface also to the left as AB dissolves into the liquid.

2.2.1. Growth of the interlayer in the case of a saturated solution

Consider first the growth of the interlayer from the saturated solution, i.e. the liquid–metal solution saturated with the dissolving metal. It

seems to be well established now that in this case the growth rate is inversely proportional to the interlayer thickness, x, available

$$\frac{dx}{dt} = \frac{k_1}{x} \tag{10}$$

where k_1 is the interlayer growth-rate constant.

The thickness of the interlayer increases in accordance with the parabolic law (initial condition: $x = 0$ at $t = 0$)

$$x = (2k_1 t)^{1/2}. \tag{11}$$

Equation 11 is valid if the interlayer growth is diffusion controlled. In other words, the overall rate of the interlayer growth is determined by the rate of atomic diffusion through the interlayer. The other processes taking place at the solid–liquid metals interface, namely, wetting, nucleating a new phase and a chemical reaction between the metals leading to the formation of an intermetallic compound, are assumed to take only a negligible portion of the total duration of the solid metal–liquid metal interaction to complete and hence these processes are considered not to affect the interlayer growth.

2.2.2. Growth of the interlayer in the case of pure liquid metal

As mentioned above, the diffusion boundary layer is rapidly formed at the solid–liquid interface in which the concentration of the dissolved metal near the solid is regarded as being equal to the saturation concentration. This means that the boundary conditions for the interlayer growth are the same in both saturated and non-saturated solutions. It seems therefore quite reasonable to suppose that the interlayer growth-rate constant, k_1, is independent of the degree of saturation of a liquid metal with a dissolving one and has the same value in both saturated and non-saturated solutions. Hence, the only distinction between these two cases is a movement of the liquid metal–interlayer interface into the solid metal side due to the interlayer dissolution in a non-saturated solution, whereas in a saturated solution this dissolution does not occur.

Then, the equation describing the growth of the interlayer under conditions of its simultaneous dissolution in liquid metal should involve a term taking into account the rate of dissolution. The linear rate of dissolution and the thickness of the interlayer dissolved can easily be found from Equations 1 and 2.

Since the concentration, c, can be given by

$$c = \frac{m}{v} \tag{12}$$

where m is the mass of the solid metal dissolved into the melt, the concentration can be written in terms of the thickness, y, of the interlayer dissolved as follows:

$$c = \frac{\rho_{int}\phi s y}{v}, \tag{13}$$

where the ρ_{int} is the density of an intermetallic compound and ϕ is the content of the more refractory metal in an intermetallic compound.

Equation 13 takes account of the fact that it is an intermetallic compound formed at the solid–liquid interface and not the solid metal itself that is being dissolved in the melt. Using Equation 13, and assuming the melt volume to be constant, we obtain from Equations 1 and 2

$$\frac{dy}{dt} = b \exp(-at) \tag{14}$$

and

$$y = \frac{b}{a}[1 - \exp(-at)], \tag{15}$$

where

$$a = \frac{ks}{v}; \quad b = \frac{c_s k}{\rho_{int}\phi}.$$

In the case of a linear dependence between the melt volume and thickness of the interlayer dissolved, Equations 14 and 15 are the same but the initial volume, v, should be replaced by the volume of saturated solution, v_s [4].

From the above, it is clear that the expression for the rate of growth of the interlayer thickness is

$$\frac{dx}{dt} = \frac{k_1}{x} - b \exp(-at). \tag{16}$$

Equation 16 expresses the difference between the rate of the interlayer growth (the first term on the right-hand side of Equation 16) and the rate of its dissolution (the second term on the right-hand side); these processes occur simultaneously.

It is difficult, if not impossible, to solve Equation 16 [5, 6]. Let us first analyse the limiting cases.

(1) If $k \to 0$ or $t \to \infty$ or $s/v \to \infty$, then $dx/dt \to$

k_1/x. Hence, in this case the thickness–time relationship is close to the parabolic law.

(2) If $s/v \to 0$, then

$$\frac{dx}{dt} \to \frac{k_1}{x} - b. \tag{17}$$

The solution to this equation is

$$\frac{k_1}{b^2} \ln \frac{1}{1 - bx/k_1} - \frac{x}{b} = t. \tag{18}$$

If

$$x = \frac{k_1}{b}, \tag{19}$$

then $dx/dt = 0$. This means that a steady state is achieved with equal rates of growth and dissolution of the interlayer. Equation 19 gives the maximum value of the interlayer thickness possible under conditions of a constant dissolution rate, b. In this case the interlayer thickness tends asymptotically to the maximum value $x_{max} = k_1/b$ but, of course, it never exceeds this value.

It should be noted that the initial increasing part of thickness–time curves is described by Equation 18. In order to show this, let us rewrite Equation 14 in the form

$$\frac{dy}{dt} = b\left(1 - at + \frac{a^2t^2}{2} - \frac{a^3t^3}{6} + \ldots\right). \tag{20}$$

If $t \to 0$, then $dy/dt \to b$ and Equation 16 is simplified to Equation 17. The limit of applicability for Equation 18 can easily be estimated because the series in Equation 20 is an alternate one. It is well known that the sum of the remainder of an alternate series does not exceed the value of the first neglected term. Hence, Equation 18 can be used until at is fairly small compared to unity.

An attempt was made to solve Equation 16 by the step-by-step approximation method, using $x_{(1)} = (2k_1t)^{1/2}$ as the first approximation [4]. Here the subscript (1) denotes the serial number of approximation. The following equation was obtained as the second approximation

$$x_{(2)} = (2k_1t)^{1/2} - \frac{b}{a}[1 - \exp(-at)]. \tag{21}$$

Equation 21 expressed the difference between the thickness of the interlayer, which would grow in a given time if the dissolution did not occur, and the thickness of the interlayer which dissolved in the same given time. Substituting Equation 21 in place of x into the denominator on the right-hand side of Equation 16, we obtain a differential equation for the third approximation

$$\frac{dx_{(3)}}{dt} = \frac{k_1}{x_{(2)}} - b\exp(-at). \tag{22}$$

But the first term of Equation 22 cannot be integrated precisely. To facilitate the solution of Equation 22 let us expand $\exp(-at)$ in the term $k_1/x_{(2)}$ in a power series and keep only two first terms of the expansion.

Then,

$$\frac{dx_{(3)}}{dt} = \frac{k_1}{x_{(1)} - bt} - b\exp(-at) \tag{23}$$

and

$$x_{(3)} = -\frac{2k_1}{b}\ln\left(1 - \frac{bt^{\frac{1}{2}}}{(2k_1)^{\frac{1}{2}}}\right) - \frac{b}{a}[1 - \exp(-at)]. \tag{24}$$

In order to reveal the distinction between Equations 21 and 24 let us rewrite Equation 24 as follows

$$x_{(3)} = \frac{2k_1}{b}\left(z + \frac{z^2}{2} + \frac{z^3}{3} + \ldots\right) - \frac{b}{a}[1 - \exp(-at)], \tag{25}$$

where $z = bt^{1/2}/(2k_1)^{1/2}; 0 \leqslant z < 1$.

If only the first term of the power series expansion is retained, then Equation 24 becomes Equation 21. But the neglected terms are positive. Hence, the first term of Equation 24 is greater than the first term of Equation 21. This means that the dissolution causes some an increase in the interlayer growth rate. This result at first sight seems improbable; however, the same conclusion can also be made immediately from Equation 16. Indeed, the dissolution decreases the value of x in the denominator and consequently increases the rate of the interlayer growth. Hence, the observed thickness is not the simple difference between the thickness of the interlayer which would grow in the absence of dissolution, i.e. in saturated solution, and the thickness of the interlayer which dissolved in a given time. For this reason, it is convenient to split the solution to Equation 16 into three parts by writing [4]

$$x = (2k_1t)^{1/2} + f(t) - \frac{b}{a}[1 - \exp(-at)]. \tag{26}$$

Each term of Equation 26 has a simple physical interpretation. The first term expresses the thickness of the interlayer which would grow in a saturated solution in a given time. The third term gives the thickness of the interlayer which was dissolved in a given time. The second term takes into account an increase in the interlayer thickness due to "the effect of dissolution" which may be called "the compensation function". It is obvious that $f(t) \geqslant 0$ for $t \geqslant 0$. One way of finding "the compensation function", $f(t)$, is apparent: write Equation 21 in the form of a power series and substitute it for x in the denominator of Equation 16. The differential equation so obtained can easily be solved by term-by-term integration. Then an approximate solution to Equation 16 is obtained in which $f(t)$ will be written in the form of a power series. By repeating this procedure, further refinement of an approximate solution can be achieved. However, there is one draw-back to this method: it is very time consuming because the more the approximate solution is refined the slower the convergence of the series.

For this reason, the numerical integration method of obtaining a solution is preferable but unfortunately it cannot be carried out at the initial condition of $x = 0$ at $t = 0$ because in this case $k_1/x \to \infty$. The "initial" condition $x = x_0$ at $t = t_0$ must therefore either be calculated from Equation 18 at small t using a known value of the dissolution rate constant or should be found experimentally. Then a time dependence of the interlayer thickness can be calculated under given conditions of interaction of a solid metal with a liquid metal.

From the above, it follows that the general solution to Equation 16 is a smooth continuous non-negative function of t which exhibits no peaks and which lies somewhere between the curves defined by Equations 11 and 18. Non-negativity of the thickness–time relationship follows from the fact that the solution to Equation 17 describing the interlayer growth at the maximum dissolution rate is non-negative. This means that the absence of the interlayer at the solid–liquid interface cannot be explained from the view-point of the diffusion processes only since the interlayer thickness has a definite value at any possible dissolution rate and $x = 0$ only if $t = 0$. In order to explain the absence of the interlayer at the interface during the interaction of a solid metal with a liquid metal the peculiarities of nucleation and the rate of chemical reaction between the metals should also be taken into account.

3. Experimental procedure

3.1. Materials and specimens

The following materials were used for the investigation.

(a) High-purity aluminium: Al: 99.995 wt %; Fe, Ti, Si, Cu and Zn $\gtrsim 1 \times 10^{-3}$ wt % each).

(b) Pure iron: Fe: 99.98 wt %; C: 4×10^{-3} wt %; N: 3×10^{-3} wt %; Al: 3×10^{-3} wt %; Ni: 1×10^{-3} wt %.

The rods, 12 mm in diameter, were prepared from the iron powder by arc-furnace melting under an argon atmosphere. Cylindrical specimens, 11.28 ± 0.01 mm in diameter and 6 mm in height, were then machined from these rods. Half of the Fe specimens was used as-received, i.e. in a rapidly solidified condition, while the remaining were subjected to a heat treatment which involved annealing in steps: 1800 sec at 1000° C and 3600 sec at 700° C. The rate of cooling from 1000 to 700° C was 0.2° C sec^{-1} and the rate of cooling from 700° C to room temperature was about 0.3° C sec^{-1}. It should be noted that, although such a heat treatment is not necessary for the present investigation, it will be necessary for future investigations. Both annealed and unannealed specimens were mechanically polished. After being polished the specimens were not annealed, thus facilitating nucleation on the solid metal surface.

Immediately before the experiment the iron specimen was pickled in a 1 : 1 v/v $HCl : H_2O$ solution, rinsed in absolute ethanol and dried. The specimen was then pressed into high-purity graphite tubes, 16.0 ± 0.2 mm in diameter, to protect the lateral surface of the specimen from the melt. Graphite had no observable effect on the rate of the interaction.

3.2. Experimental details.

A rapid-quenching device employed in this work has been described in detail elsewhere [7]. The experimental runs were performed by the rotating disc technique.

24.0 g of aluminium was melted under a flux (KCl, 40 wt %; LiCl, 30 wt %; NaCl, 10 wt %; Na_3AlF_6, 5 wt %; $ZnCl_2$, 15 wt %) into a 26 mm inside diameter alumina crucible. The flux was used both to prevent the oxidation of the aluminium and to pre-heat the iron specimen up to

the temperature of the investigation. For the latter purpose, the specimen was dipped into the crucible so that it was beneath the surface of the flux but above the surface of aluminium. Fe dissolved slightly in the flux. To ensure the uniform dissolution of the solid metal surface in the flux the iron specimen was rotated (rotation rate, $\omega = 6.45\,\text{rad sec}^{-1}$) during pre-heating. It should be noted that specimen dissolution in the flux caused a negligible contamination of the aluminium melt (less than $0.05\,\text{kg m}^{-3}$ Fe).

When the temperature had equilibrated (after 400 to 500 sec) the rotating iron specimen was dipped into the aluminium melt so that the distance between the crucible bottom and the disc surface was 15.0 ± 0.5 mm. At the end of the experiment, the crucible together with the melt and the iron specimen was "shot" into water to arrest the reactions at the interface. Note that the specimen continued to be rotated until crystallization of the melt. It took between 2 and 3 sec for the aluminium specimen to cool from the investigation temperature to room temperature.

The experiments were performed at $700 \pm 5°$ C for 50 to 300 sec. The angular speed of the disc rotation was $24.0 \pm 0.1\,\text{rad sec}^{-1}$.

After the experiment, the bimetallic specimen obtained was cut along the cylinder axis, ground and both polished and etched electrolytically using the "Elypovist" electropolishing apparatus ("Carl Zeiss", DDR) and special electrolytes [8]. Metallographic and X-ray techniques were used to investigate the interlayer.

The aluminium part of the specimen was analysed to find its Fe content by a photometric method. The relative error of determination did not exceed ± 5%.

4. Results and discussion

4.1. Dissolution kinetics

The dissolution data obtained is shown in Fig. 2. The exponential law of dissolution, Equation 2, can be written as

$$\ln \frac{c_s}{c_s - c} = k \frac{st}{v}. \qquad (27)$$

Hence, a plot of $\ln c_s/c_s - c$ against st/v should be a straight line, as confirmed in Fig. 3. It is clear that, in this case, the dissolution rate constant and the diffusion coefficient could be calculated using Equations 27 and 9, respectively. The following values were used for calculations:

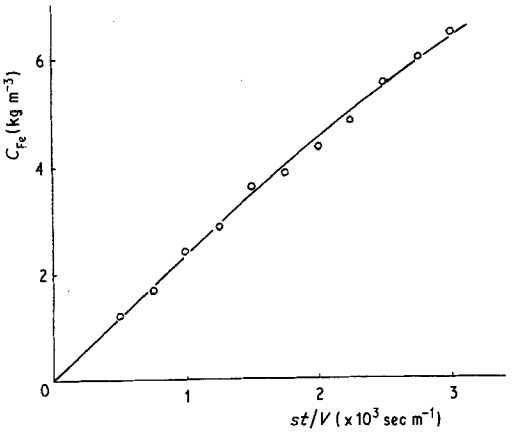

Figure 2 Concentration of iron in aluminium plotted against st/v.

(a) $c_s = 60 \pm 3\,\text{kg m}^{-3}$, from [9];
(b) $s/v = 10.0 \pm 0.2\,\text{m}^{-1}$;
(c) $\nu = 4.79 \times 10^{-7}\,\text{m}^2\,\text{sec}^{-1}$, from [10];
(d) $\omega = 24.0 \pm 0.1\,\text{rad sec}^{-1}$.

The density of the Fe–Al melts depends only to a small extent on the Fe content. For this reason, the density of the aluminium melt, ρ_{Al}, was assumed to be constant up to the saturation concentration, $\rho_{Al} = 2.40 \times 10^3\,\text{kg m}^{-3}$ [11].

The following value of the dissolution rate constant, k, was obtained from the experimental data by the least-squares fit method (0.95 confidence limit):

$$k = (3.8 \pm 0.1) \times 10^{-5}\,\text{m sec}^{-1}.$$

The approximate value of the diffusion coefficient, D, was first calculated from Equation 8; the Schmidt number and the correction factor, I, [3] were then found, and the precise value of D was calculated from Equation 9 giving

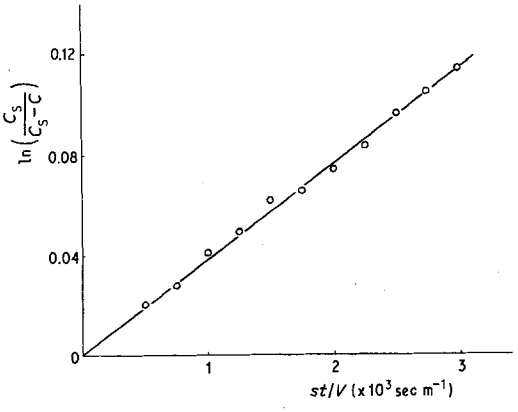

Figure 3 Ln $c_s/c_s - c$ plotted against st/v for the data of Fig. 2.

$$D = 1.24 \times 10^{-9} \text{m}^2 \text{sec}^{-1}.$$

The relative error of determination was estimated as ± 10%.

It should be noted that this value represents the coefficient of diffusion of the Fe-atoms through the diffusion boundary layer. Hence, its value is closer to that of the coefficient of diffusion of the Fe atoms into the Fe-saturated aluminium melt than it is to that of the Fe atoms into pure liquid aluminium because the average Fe-concentration in the diffusion boundary layer varies with time from $c_s/2$ up to c_s if the initial iron concentration in the melt is zero. Moreover, a linear dependence of $\ln c_s/c_s - c$ on st/v for a wide concentration range (the concentration varied from 0.01 to $0.75 c_s$) which has been observed for the aluminium–transition metal (Ti, V, Cr, Fe, Co, Nb, Mo, Ta, W) systems [7, 9], indicates that D is independent of concentration or, alternatively, that D and δ change in such a way that k remains a constant. The latter assumption seems improbable; it is not surprising that D has been found to be independent of concentration in the systems listed above, indeed, in these systems the saturation concentration is comparatively low and, hence, an appreciable influence of concentration on the diffusion coefficients would not be expected.

4.2. Growth of the Fe_2Al_5 interlayer

In the Fe-saturated aluminium melt the Fe_2Al_5 interlayer growth follows parabolic-law kinetics [12]. The presence of parabolic-law kinetics indicates control by diffusion through the interlayer thickness and not control by either interface reaction. Interface control would give a linear time dependence for the interlayer thickness.

A single-phase interlayer consisting of the Fe_2Al_5 intermetallic compound and having a very distinctive, tongue-like structure, grows at the solid iron–liquid aluminium interface at 700° C, see Fig. 4.

The first experiment conducted was a control: the rotating iron specimen (after pre-heating) was immersed in the aluminium melt and immediately the crucible was "shot" into water. Examination of the bimetallic specimen obtained in such a way showed that an Fe_2Al_5 interlayer about 1 μm thick had been formed at the Fe–Al interface. This shows that wetting and nucleation were relatively fast processes and took not more than between 1 and 3 sec to complete. This time, 1 to 3 sec, is a small portion of the total duration of the experiment, 50 to 300 sec, and the interlayer thickness formed in this time, 1 μm, is a small portion of the interlayer thickness measured, 40 to 90 μm.

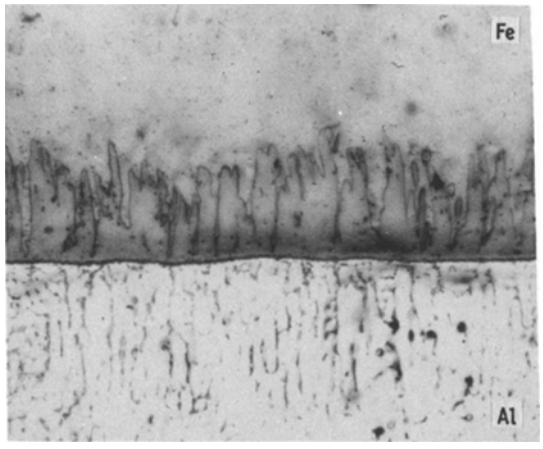

Figure 4 Micrograph of the Fe–Al interface. Temperature = 700° C; Rotation rate = 24.0 rad sec^{-1}; t = 250 sec.

The experimental points are shown in Fig. 5 (circles). The average value of the maximum height of the Fe_2Al_5 crystallites was used as a measure of the interlayer thickness. The relative error of determination of the interlayer thickness was about ± 15%.

The theoretical thickness–time relationship was calculated from Equation 18 using the following values:

(a) $k_1 = 1.0 \times 10^{-10} \text{m}^2 \text{sec}^{-1}$, from [12];

(b) $\rho_{\text{int}} = (4.1 \pm 0.1) \times 10^3 \text{kg m}^{-3}$

(c) $\phi = 0.453$ (the mass fraction of Fe in Fe_2Al_5).

The linear rate of dissolution, $b = 1.16 \times 10^{-6} \text{m sec}^{-1}$, was taken as an arithmetic mean at the end of the b values at the start, $t = 0$, and at the end, $t = 300$ sec, of the experiment ($b_{t=0} = c_s k/\rho_{\text{int}}\phi = 1.23 \times 10^{-6} \text{m sec}^{-1}$, $b_{t=300} = b_{t=0} \exp(-at) = 1.10 \times 10^{-6} \text{m sec}^{-1}$). It is seen that the linear rate of dissolution, b, can be considered to be constant within ± 6%, and, hence, Equation 18 should describe the Fe_2Al_5 interlayer growth with a sufficient degree of accuracy. The calculated curve is plotted in Fig. 5 (Curve 2); the functions $x_{(1)} = (2k_1 t)^{1/2}$, (Curve 1); $x_{(2)} = (2k_1 t)^{1/2} - (b/a)[1 - \exp(-at)]$, (Curve 3); and $y_{Fe_2Al_5} = (b/a)[1 - \exp(-at)]$, (Curve 4), are also given for comparison.

From the presented data it can be concluded that the agreement between the theoretical plot

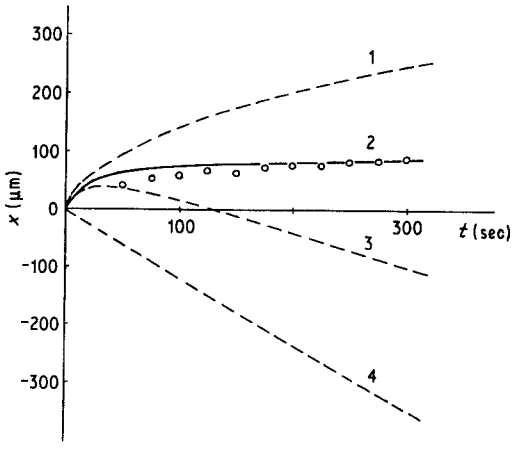

Figure 5 Thickness–time relationships: (1) $x_{(1)} = (2k_1t)^{1/2}$, from Equation 11; (2) $(k_1/b^2)\ln\{1/[1-(bx/k_1)]\} - x/b = t$, from Equation 18; (3) $x_{(2)} = (2k_1t)^{1/2} - (b/a)[1-\exp(-at)]$, from Equation 21; (4) $y_{Fe_2Al_5} = (b/a)[1-\exp(-at)]$, from Equation 15. Open circles are the experimental determined points.

(Curve 2 in Fig. 5) and the experimental points (open circles in Fig. 5) is satisfactory. A certain disagreement is observed near the initial increasing part of the curve. The reasons for this are the following.

(1) It was assumed that the linear rate of dissolution was constant whereas it decreased almost linearly from $b_{t=0}$ to $b_{t=300}$. As a result, the theoretical curve over-estimates the interlayer thickness for the first half (0 to 150 sec) and underestimates it for the second half (150 to 300 sec). This reason alone, of course, cannot lead to the observed disagreement since the error introduced by this assumption is small compared to the experimental errors (6 and 15%, respectively).

(2) There is an anisotropy of the Fe_2Al_5 crystallite growth. Each tongue-like crystallite (see Fig. 4) represents a single crystal, the axis of which coinsides with the c-axis of the unit cell [12]. The maximum value of the Fe_2Al_5 crystallite growth-rate is observed in the direction of the c-axis; this is due to the peculiarities of the Fe_2Al_5 lattice structure (for details see [12]. However, the maximum values of the growth rates of the Fe_2Al_5 crystallites are observed only if the angles between the c-axis and the original Fe–Al interface are 90°. If these angles considerably differ from 90° then neighbouring crystallites hinder each other's growth. It is clear that at the early stages of the interaction a large number of the spontaneously orientated Fe_2Al_5 nuclei was formed on the iron surface and this was one reason for a decrease of the growth-rate constant, k_1, from its maximum value.

During dissolution, the unfavourably orientated Fe_2Al_5 nuclei gradually disappear whereas the favourably orientated ones continue to grow. As a result, the interlayer assumes the tongue-like morphology and k_1 attains the maximum value. This is another aspect of the influence of dissolution on the Fe_2Al_5 interlayer growth.

5. Conclusions and remarks

The above consideration is based upon Fick's first law and assumes a linear change of concentration with distance into both the interlayer and the diffusion boundary layer. Hence, the results presented here would be valid for solid–liquid systems in which:

(a) low solubility of a solid in a liquid is observed;

(b) an intermetallic compound having a narrow homogeneity range is formed.

If these conditions are satisfied, then the complete thickness–time relationship can be calculated from Equation 16 knowing the following:

(1) the interlayer growth-rate constant in the saturated melt,

(2) the melt density,

(3) the saturation concentration,

(4) the density of the intermetallic compound,

(5) the solid metal surface area exposed to the liquid metal attack,

(6) the melt volume,

(7) the dissolution rate constant,

(8) the content of the more refractory metal in the intermetallic compound.

The related parameters, namely, the degree of saturation of the melt with the dissolving metal and the thickness of the solid metal dissolved can also be determined using Equations 2 and 15, respectively. In the latter case, the product $\rho_{int}\phi$ should be replaced by the solid metal density.

Equation 16 gives the upper limit for the interlayer thickness. The interlayer thickness observed in a real metallic system cannot exceed the value predicted by Equation 16 but it can be far less than the predicted value if the wetting, nucleating or chemical reaction between the metals is an insufficiently fast process.

The main conclusion following from the presented results is that the interlayer growth cannot be considered as independent of its dissolution (compare the theoreticaly determined curves,

Curves 2 and 3, in Fig. 5, with the experimentally determined points, open circles in Fig. 5). Hence, it is impossible to avoid the formation of the interlayer by increasing the dissolution rate if the interlayer growth is controlled by atomic diffusion. The reasons for the absence of the interlayer during the solid metal–liquid metal interaction lie in the peculiarities of nucleation or chemical reaction between the metals. It should be emphasized that the absence of the interlayer in the early stages of the interaction and its subsequent formation does not affect the dissolution kinetics [7].

Two remarks concerning the rotating disc method should be made.

(a) The formation of the interlayer deterioriates to a large extent the result obtained by this method if the weight loss of the solid specimen is used to control the run of the dissolution process and if the duration of experiment is short. In this case, the weight loss due to the dissolution and an increase in the specimen weight due to the interlayer formation are of the same order of magnitude (this can be seen, for example, from Curves 2 and 4, in Fig. 5). If the experimental parameters remain unchanged during the investigation, then a good reproducibility of results may be observed, since this error is systematic, but it is clear that the final result will not be correct. The same can be said about the method of control based on measurements of the specimen dimensions. A change in the specimen dimensions can be measured only to within an accuracy of plus or minus the available interlayer thickness. These observations were first noted as far back as 1970 [13]. Since that time a number of studies have been performed, using the rotating disc method, but in only a few of these were the above points taken into account. This is one of the reasons for the discrepancies in the results obtained to date.

(2) When $c \to c_s$, then even a comparatively small error in the determination of the concentration results in large error in calculating the dissolution rate constant and, as a consequence, in the value of the diffusion coefficient. This is due to the small value of the denominator $(c_s - c)$ in Equation 27. For this reason, the data obtained at concentrations close to the saturation concentration should be used with a great care.

The concentration range from $0.01\,c_s$ to $0.75\,c_s$ is the optimum one for calculating the dissolution rate constants from the data obtained by the rotating disc method; of course, these limits are somewhat arbitrary. In general, the lower limit is determined by the sensitivity whereas the upper limit is determined by the accuracy of the method which is employed to control the run of the dissolution process.

References

1. L. L. BIRCUMSHAW and A. C. RIDDIFORD, *Quart. Rev.* **6** (1952) 157.
2. V. G. LEVICH, "Physicochemical Hydrodynamics" (Fizmatgiz, Moscow, 1959), in Russian.
3. T. F. KASSNER, *J. Electrochem. Soc.* **114** (1967) 689.
4. V. I. DYBKOV, *Zh. Fiz. Khimii* **53** (1979) 2868.
5. E. KAMKE, "Differential Gleichungen, Lösungsmethoden und Lösungen: 1, Gewöhnlich Differential Gleichungen" (Leipzig, 1959), in German.
6. A. K. MARISHKIN, *Avtom. Svarka* **12** (1974) 61.
7. V. N. YEREMENKO, Ya. V. NATANZON and V. I. DYBKOV, *J. Less-Common Metals* **50** (1976) 29.
8. V. I. DYBKOV, *Poroshkovaya Metallurgiya* **3** (1980) 54.
9. V. N. YEREMENKO, Ya. V. NATANZON and V. P. TITOV, *Fiz.-Khim. Mechanika Materialov* **6** (1978) 3.
10. E. S. LEVIN, *Izv. Akad. Nauk SSSR, Met.* **5** (1971) 72.
11. A. E. VOL, "Structure and Properties of Binary Metallic Systems" (Fizmatgiz, Moscow, 1959), in Russian.
12. Th. HEUMANN, S. DITTRICH, *Z. Metallkunde* **50** (1959) 617.
13. V. N. YEREMENKO and Ya. V. NATANZON, *Poroshkovaya Metallurgiya* **8** (1970) 39.

Received 6 March and accepted 22 September 1980.